A Comparison Scheme of Dynamic Voltage for Smart Electric Grid Stabilization and Efficient Utilization using FACTS

V.Lakshma Naik
Department of Electrical and Electronics Engineering
BITIT-Hindupur,Ananthapuramu, Andhra Pradesh, India.

Abstract - This paper presents a Comparision Scheme Of Dynamic Voltage For Smart Electric Grid Stabilization And Effiient Utilization Using FACTS. Modulated Power Filter Compensator (MPFC) for the distribution networks with dispersed renewable wind energy interfaced. A tri-loop error driven controller is used to adjust the PWM switching of the modulated power filter compensator. Full power factor correction and power quality improvement is validated under different operation conditions, like load switching and wind velocity excursions.
The MPFC is controlled by a a Comparision Scheme Of Dynamic Voltage For Smart Electric Grid Stabilization And Effiient Utilization Using FACTS. The MATLAB digital simulation models of the proposed MPFC scheme has been fully validated for effective power quality (PQ) improvement, voltage stabilization, power factor correction and transmission line loss reduction. The proposed FACTS based scheme can be extended to distributed renewable energy interface and utilization systems and can be easily modified for other specific stabilization, compensation requirements, voltage regulation and efficient utilization.

Keywords – Dynamic Voltage Stabilization, FACTS, MPFC, Smart Electric Grid.

I. INTRODUCTION

A power quality problem is defined as any variation in voltage, current or frequency that may lead to an equipment failure or malfunction. In a modern electrical distribution system, there has been a sudden increase of nonlinear loads, such as power supplies, rectifier equipment used in telecommunication networks, domestic appliances, adjustable speed drives, etc. These power-electronic-based loads offer highly nonlinear characteristics. Due to their non-linearity, the loads are simultaneously the major causes and the major victims of power quality problems.

During the last two decades, renewable wind energy has become increasingly popular as a consequence of strong ecological concerns and appealing advantages with regard to economical energy solutions in remote communities. Furthermore, with very large wind farms emerging, the dispersed renewable wind energy is required to be fully connected to the electrical distribution networks. However, the integration of dispersed renewable wind energy will pose a great challenge to the power quality in the distribution networks when the weak nature of the grid in remote areas and the uncertainty of wind are taken into consideration.

Wind is an abundant renewable source of energy, which is usually obtained by converting part of the kinetic energy in the moving air into electricity. Wind renewable energy is also a clean energy source that is, operating without producing carbon dioxide, sulfur dioxide, particulates or any other type of air pollution. Demand for electrical energy from renewable sources is rapidly increasing as industrialized societies are becoming more aware of and concerned about fossil fuel shortage and environmental impacts. Besides hydro-power, which is already well established, wind energy is by far one of the most technically advanced and promising renewable energy sources. In many countries, the potential for wind energy production exceeds by far the local consumption of electricity. By 2005, the worldwide capacity had been increased to 58,982 megawatts and the World Wind Energy Association expects 120,000 MW to be installed globally by 2010. Germany is the leading producer of wind power with a capacity of 18,428 megawatts in 2005, which accounts for 6% of German electricity in the same year.

The applications of FACTS based schemes for standalone wind energy were studied. By far, the Static VAR Compensator (SVC) has been the extensively utilized FACTS based devices that can maintain a constant voltage by continuously adjusting reactive power flow through the grid-connected WECS. To ensure proper operation of the SVC, various mathematical models and control strategies have been developed. Numerous studies have been performed dealing with the steady state and transient condition using a number of simulation platforms. E.S. Abdin

proposed two controllers for the SVC and the digital simulation results have validated good damping and fast system recovery from different types of large disturbances and excursions. A Harmonic mitigation scheme using an Active Power Filter for a wind energy generation system was also investigated. A Unified Power Flow Controller (UPFC) for power flow control and voltage regulation under different types of wind speed changes was studied.

This paper focuses on the impact of a dispersed renewable wind energy scheme integrated into distribution network on operation, voltage and frequency stabilization, as well as the need of novel FACTS stabilization devices and control strategies such as the low cost Modulated Power Filter Compensator (MPFC) developed by the first author. Comparing with the conventional FACTS devices, the novel MPFC has the advantage of simple structure and low cost, since no line commuted converter is involved in the MPFC scheme. In this paper, the effectiveness of the proposed MPFC scheme for both power quality improvement and power factor correction is fully validated using MATLAB/SIMULINK software environment.

II. PROPOSED ALGORITHM

2. Wind Energy Conversion System(WECS) of Power Generation System

The electrical power generation structure contains both electromagnetic and electrical subsystems. Besides the electrical generator and power electronics converter it generally contains an electrical transformer to ensure the grid voltage compatibility. However, its configuration depends on the electrical machine type and on its grid interface (Heier 2006).

2.1. Variable-speed WECS

Variable-speed wind turbines are currently the most used WECS. The variable speed operation is possible due to the power electronic converters interface, allowing a full (or partial) decoupling from the grid. The doubly-fed-induction-generator (DFIG)-based WECS, also known as improved variable-speed WECS, is presently the most used by the wind turbine industry.

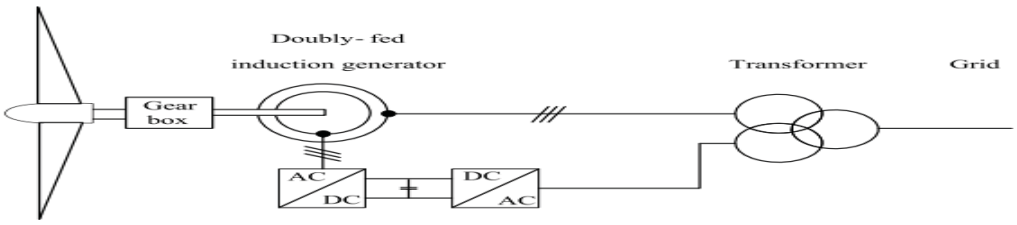

Figure 2.1.a) General structure of an improved variable-speed WECS

The DFIG is a WRIG with the stator windings connected directly to the three phase, constant-frequency grid and the rotor windings connected to a back-to-back (AC–AC) voltage source converter (Akhmatov 2003; Ackermann 2005). Thus, the term “doubly-fed” comes from the fact that the stator voltage is applied from the grid and the rotor voltage is impressed by the power converter. This system allows variable-speed operation over a large, but still restricted, range, with the generator behavior being governed by the power electronics converter and its controllers.

The power electronics converter comprises of two IGBT converters, namely the rotor side and the grid side converter, connected with a direct current (DC) link. Without going into details about the converters, the main idea is that the rotor side converter controls the generator in terms of active and reactive power, while the grid side converter controls the DC-link voltage and ensures operation at a large power factor. The stator outputs power into the grid all the time. The rotor, depending on the operation point, is feeding power into the grid when the slip is negative (over synchronous operation) and it absorbs power from the grid when the slip is positive (sub-synchronous operation). In both cases, the power flow in the rotor is approximately proportional to the slip (Lund et al. 2007). The size of the converter is not related to the total generator power but to the selected speed variation range. Typically a range of r40% around the synchronous speed is used (Akhmatov 2003). DFIG-based WECS are highly controllable, allowing maximum power extraction over a large range of wind speeds.

Furthermore, the active and reactive power control is fully decoupled by independently controlling the rotor currents. Finally, the DFIG-based WECS can either inject or absorb power from the grid, hence actively participating at voltage control. Full variable-speed WECS are very flexible in terms of which type of generator is used. It can be equipped with either an induction (SCIG) or a synchronous generator. The synchronous generator can be either a wound-rotor synchronous generator (WRSG) or a permanent-magnet synchronous generator (PMSG), the latter being the one mostly used by the wind turbine industry. The back-to-back power inverter is rated to the generator power and its operation is similar to that in DFIG-based WECS. Its rotor-side ensures the rotational speed being adjusted within a large range, whereas its grid-side transfers the active power to the grid and attempts to cancel the reactive power consumption. This latter feature is important especially in the case of SCIG-equipped WECS.

The PMSG is considered, in many research articles, a good option to be used in WECS, due to its self-excitation property, which allows operation at high power factor and efficiency (Alatalo 1996). PMSG does not require energy supply for excitation, as it is supplied by the permanent magnets.

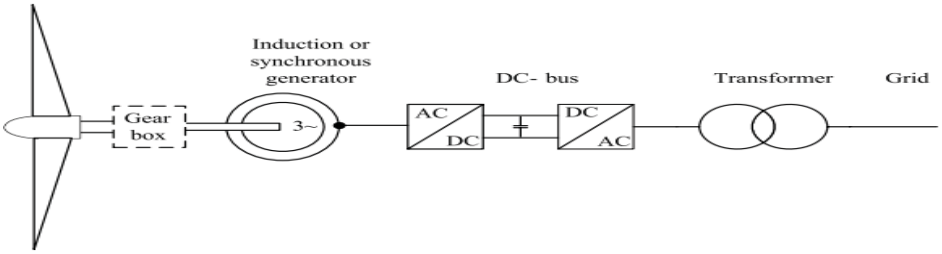

Figure 2.1.b) General structure of a full variable-speed WECS

The stator of a PMSG is wound and the rotor has a permanent magnet pole system. The salient pole of PMSG operates at low speeds, and thus the gearbox can be removed. This is a big advantage of PMSG-based WECS as the gearbox is a sensitive device in wind power systems. The same thing can be achieved using direct driven multi pole PMSG with large diameter. The synchronous nature of PMSG may cause problems during start-up, synchronization and voltage regulation and they need a cooling system, since the magnetic materials are sensitive to temperature and they can lose their magnetic properties if exposed to high temperatures (Ackermann 2005).

III. SIMULATION RESULTS

The Mat lab digital simulation results using MATLAB/SIMULINK/Sims-Power Software Environment for the proposed MPFC scheme under three different study cases are:

3.1 Normal Loading Operation Case

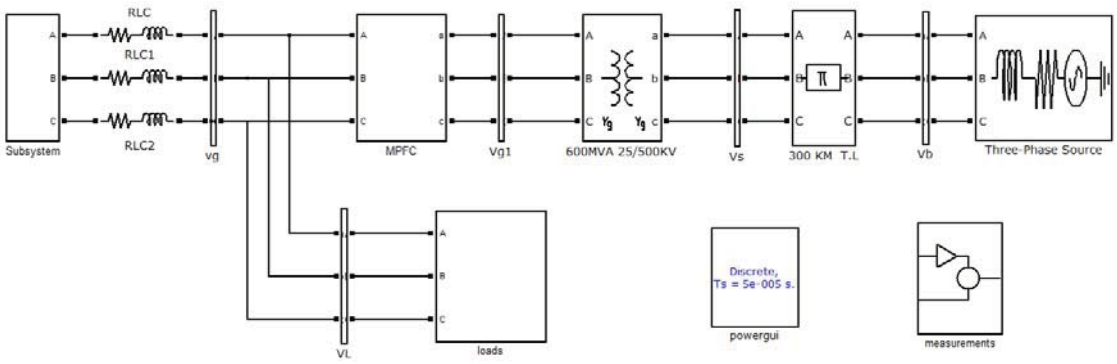

Figure 3.1: Simulation Circuit of Proposed Facts Based Dynamic Voltage Compensation **Scheme**

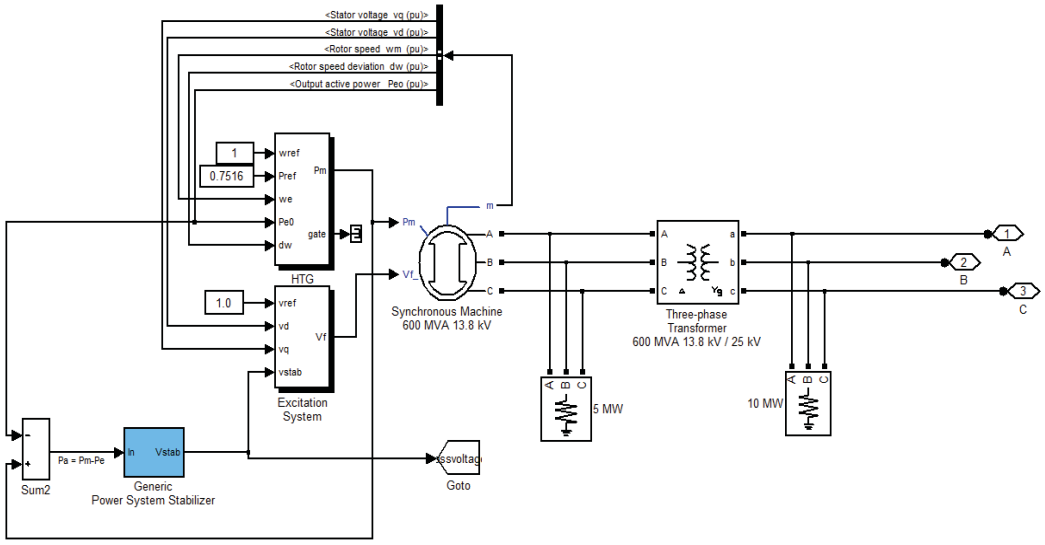

Figure 3.2: Simulation Circuit of Wind Energy Conversion System

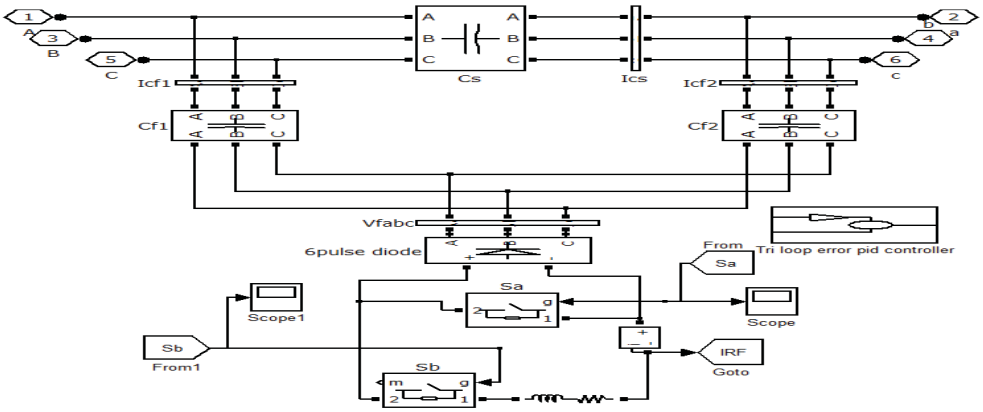

Figure 3.3: Simulation Circuit of Proposed A Novel Modulated Power Filter Compensator

This scheme of MPFC structure comprises a series fixed capacitor bank and two shunt fixed capacitor banks. The low cost modulated dynamic series-shunt power filter and compensator is a switched type filter, used to provide measured filtering in addition to reactive compensation.

The modulated power filter and compensator is controlled by the on-off timing sequence of the pulse width modulation (PWM) switching pulses that are generated by the dynamic tri loop error driven dynamic modified PID controller.

3.1.1 Generator bus

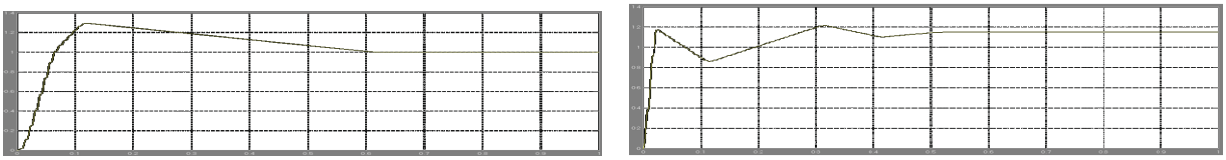

Figure 3.4: the RMS voltage at AC generator bus under normal operation without and with MPFC

Figure 3.4 represents the waveform of RMS voltage at AC generator bus under normal operation without and with MPFC. Here we are representing the Time (sec) on X-axis and RMS Voltage (Pu) on Y-axis.

In fig 3.4(a), initially (t=0sec) there is no load so that pu RMS voltage increases from 0 to 1.3 pu RMS voltage. Linear and nonlinear load is on at 0.1sec so that pu RMS voltage is reduced 1.3 pu to 1pu RMS voltage between 0.1 to 0.6 sec after that pu RMS voltage to be constant.

In fig 3.4(b), At t=0sec there is no load so that pu RMS voltage increases from 0 to 1.2 pu RMS voltage, system pu RMS voltage is unbalanced between 0.01sec to 0.5sec due to linear and nonlinear load pu RMS voltage to 1.1 pu is stabilize at 0.5 sec due to MPFC.

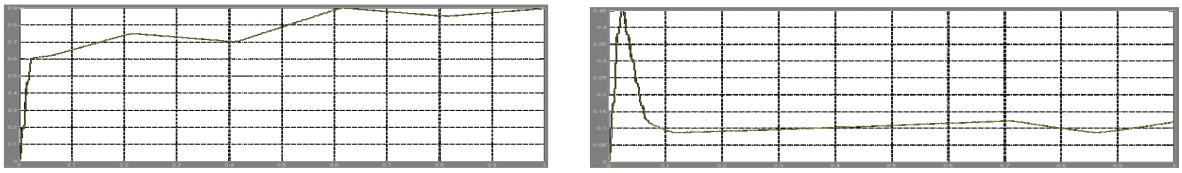

Figure 3.5: the RMS current at AC generator bus under normal operation without and with MPFC

Figure 3.5 represents the waveform of RMS Current at AC generator bus under normal operation without and with MPFC. Here we are representing the Time (sec) on X-axis and RMS Current (Pu) on Y-axis.

In fig 3.5(a), initially (t=0sec), pu RMS current increases from 0 to 0.6 pu RMS current. Linear and nonlinear load is on at 0.1sec so that pu RMS current is increased 0.6 pu to 0.9pu between 0.1 to 0.6 sec after pu RMS current to be approximately constant.

In fig 3.5(b), At t=0sec, pu RMS current losses increases from 0 to 0.45 pu RMS current due to linear and nonlinear load & pu RMS current is unbalanced between 0.01sec to 0.1sec, due to MPFC pu RMS current losses is decreased and stabilize at 0.1sec.

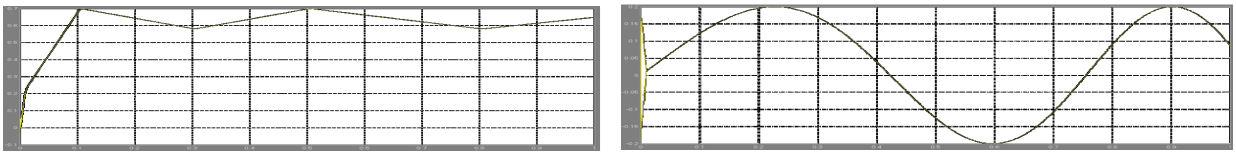

Figure 3.6: The reactive power at AC generator bus under normal operation without and with MPFC

Figure 3.6 represents the waveform of Reactive power at AC generator bus under normal operation without and with MPFC. Here we are representing the Time (sec) on X-axis and Reactive power (Pu) on Y-axis.

In fig 3.6(a), initially (t=0sec) pu reactive power losses increases from 0 to 0.7 pu due to Linear and nonlinear load and stabilized.

In fig 3.6(b), pu Reactive power losses is increases from 0 to 0.2 pu due to linear and nonlinear load, pu reactive power is unbalanced pu reactive power losses is decreased to fully by due to MPFC.

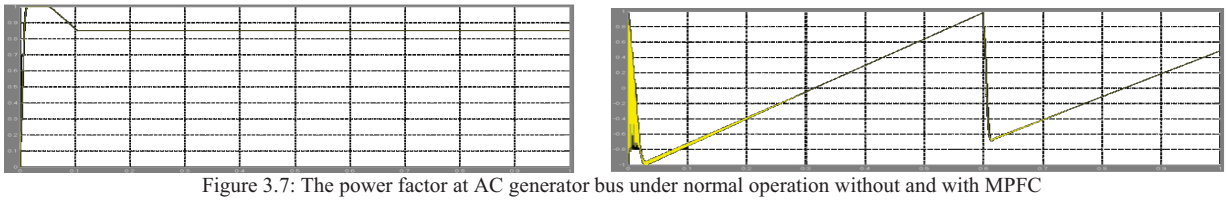

Figure 3.7: The power factor at AC generator bus under normal operation without and with MPFC

Figure 3.7 represents the waveform of Power factor at AC generator bus under normal operation without and with MPFC.Here we are representing the Time (sec) on X-axis and Power factor on Y-axis.

In fig 3.7 (a), pu power factor is decreased to 0.85 pu between 0.01 to 0.1 sec due to unbalanced load after pu power factor to be constant.

In fig 3.7 (b), pu power factor is unbalanced due to linear and nonlinear load, and pu power factor is increased to unity due to MPFC at 0.6 sec.

3.1.2 Load bus

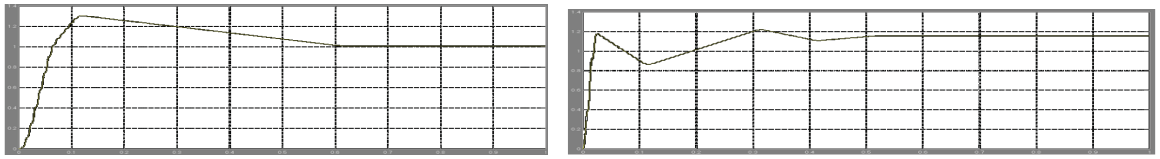

Figure 3.8: The RMS voltage at AC load bus under normal operation without and with MPFC

Figure 3.8 represents the waveform of RMS voltage at AC load bus under normal operation without and with MPFC.Here we are representing the Time (sec) on X-axis and RMS Voltage (Pu) on Y-axis.

In fig 3.8 (a), initially (t=0sec) there is no load so that pu Vrms increases from 0 to 1.2 pu Vrms. Linear and nonlinear load is on at 0.1sec so that pu Vrms is reduced 1.3 pu to 1pu Vrms between 0.1 to 0.6 sec after that pu Vrms to be constant.

In fig 3.8 (b), At t=0sec, there is no load so that pu Vrms increases from 0 to 1.2 pu Vrms, system pu Vrms is unbalanced between 0.01sec to 0.5sec due to linear and nonlinear load and pu Vrms is stabilize at 0.5 sec due to MPFC.

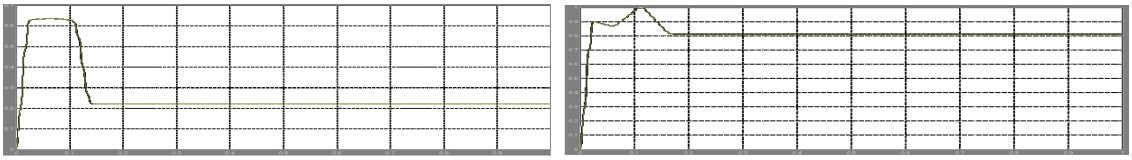

Figure 3.9: The RMS current at AC load bus under normal operation without and with MPFC

Figure 3.9 represents the waveform of RMS Current at AC load bus under normal operation without and with MPFC.Here we are representing the Time (sec) on X-axis and RMS Current (Pu) on Y-axis.

In fig 3.9 (a), initially (t=0sec) pu RMS current increases from 0 to 0.6 pu RMS current. Linear and nonlinear load is on at 0.1sec so that pu RMS current is decreased 0.6 pu to 0.9pu RMS current between 0.01 to 0.1 sec after pu RMS current to be approximately constant.

In fig 3.9 (b), At t=0sec, there is no load so that pu RMS current increases from 0 to 0.9 pu RMS current due to linear and nonlinear load pu RMS current is unbalanced between 0.01sec to 0.1sec due to MPFC pu RMS current is stabilize at 0.2sec.

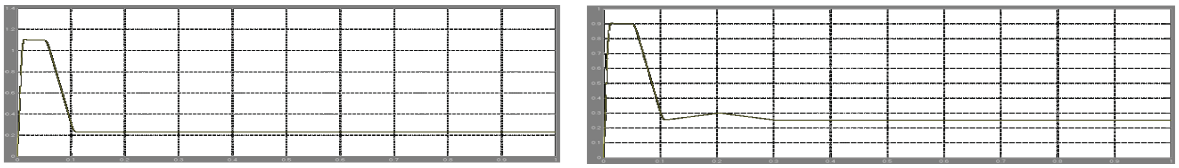

Figure 3.10: The reactive power at AC load bus under normal operation without and with MPFC

Figure 3.10 represents the waveform of Reactive power at AC load bus under normal operation without and with MPFC.Here we are representing the Time (sec) on X-axis and Reactive power (Pu) on Y-axis.

In fig 3.10 (a), initially (t=0sec), pu reactive power increases from 0 to 1.1 pu reactive power. linear and nonlinear load is on at 0.1sec so that pu reactive power is decreased 1.1 pu to 0.2 pu reactive power between 0.01 to 0.1 sec after reactive power pu to be constant.

In fig 3.10 (b), pu Reactive power increases from 0 to 0.9 pu reactive power due to linear and nonlinear load pu reactive power is unbalanced between 0.01sec to 0.1sec, due to MPFC pu reactive power is decreased.

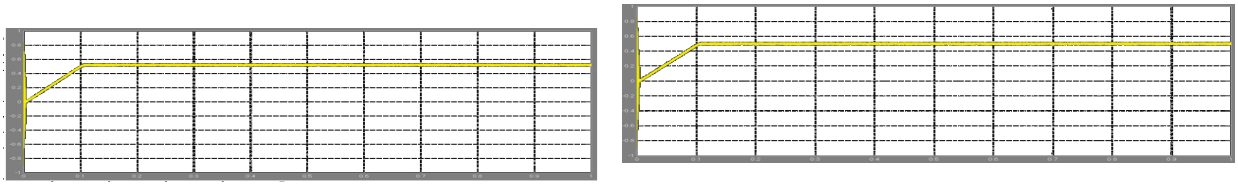

Figure 3.11: The power factor at AC load bus under normal operation without and with MPFC

Figure 3.11 represents the waveform of Power factor at AC load bus under normal operation without and with MPFC.Here we are representing the Time (sec) on X-axis and Power factor In on Y-axis.

fig 3.11 (a), pu power factor is increased to 0.5 pu between 0.01 to 0.1 sec due to unbalanced load after pu power factor to be constant.

In fig 3.11(b), pu power factor is unbalanced due to linear and nonlinear load, and pu power factor is increased to unity due to MPFC at 0.6 sec.

3.1.3 Infinite bus

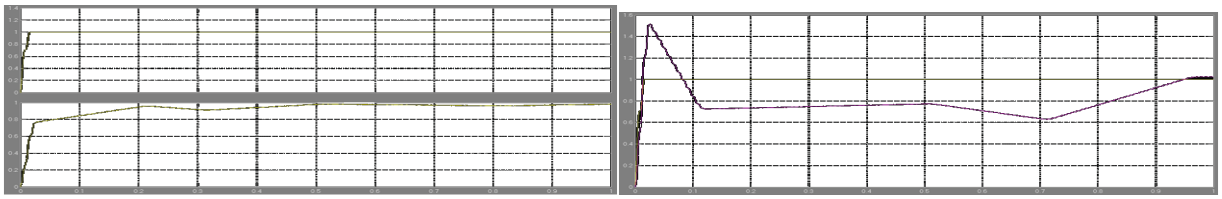

Figure 3.12:The RMS voltage and current at the infinite bus under normal operation without & with MPFC

Figure 3.12 represents the waveform at AC infinite bus under normal operation without MPFC.Here we are representing the Time (sec) on X-axis and voltage and current on Y-axis.

Figure 3.13 represents the waveform at AC infinite bus under normal operation with MPFC.Here we are representing the Time (sec) on X-axis and voltage and current on Y-axis.

In fig 3.13 (a), initially (t=0sec) there is no load so that pu Vrms increases from 0 to 1 pu Vrms. Linear and nonlinear load is on at 0.1sec so that pu Vrms to be constant.

In fig 3.13 (b), initially (t=0sec), there is no load so that pu RMS current increases from 0 to 1.5 pu RMS current. Linear and nonlinear load is on at 0.1sec so that pu RMS current is decreased 1.5 pu to 0.8pu RMS current between 0.01 to 0.1 sec after pu RMS current to be approximately constant.

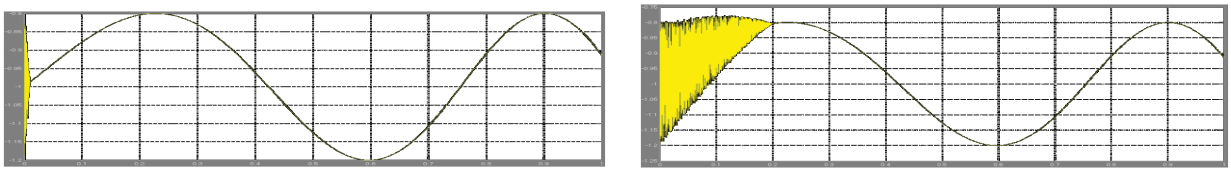

Figure 3.14: The reactive power at the infinite bus under normal operation without and with MPFC

Figure 3.14 represents the waveform at AC infinite bus under normal operation with MPFC.Here we are representing the Time (sec) on X-axis and voltage and current on Y-axis.

In fig 3.14 (a), initially (t=0sec) there is no load so that pu reactive power increases from 0 to 1.1 pu reactive power. Linear and nonlinear load is on at 0.1sec so that pu reactive power is decreased 1.1 pu to 0.2 pu reactive power between 0.01 to 0.1 sec after reactive power pu to be constant.

In fig 3.14 (b), pu Reactive power increases from 0 to 0.9 pu reactive power due to linear and nonlinear load pu reactive power is unbalanced between 0.01sec to 0.1sec, due to MPFC reactive power pu is decreased.

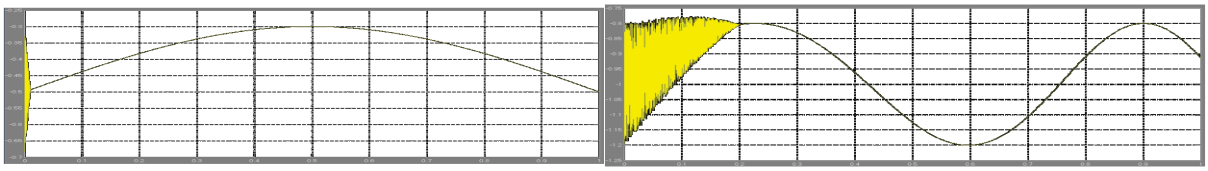

Figure 3.15: The power factor at the infinite bus under normal operation without and with MPFC

Figure 3.15 represents the waveform at AC infinite bus under normal operation with MPFC.Here we are representing the Time (sec) on X-axis and power factor on Y-axis.

In fig 3.15 initially (t=0sec) there is no load so that power factor increases from 0 to 0.5 pu power factor. Linear and nonlinear load is on at 0.1sec so that pu power factor is increased between 0.01 to 0.1 sec after power factor pu to be constant.

At t=0sec there is no load so that pu power factor increases from 0 to 0.5 pu power factor due to linear and nonlinear load pu power factor is unbalanced between 0.01sec to 0.1sec due to MPFC power factor pu is improved.

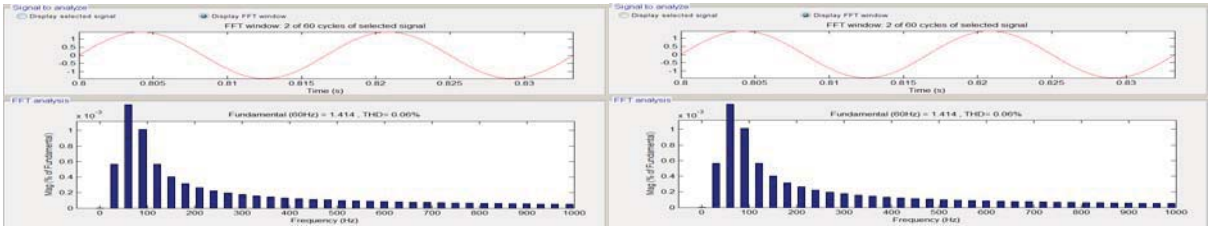

Figure 3.16: THD and FFT of voltage waveforms at the infinite bus with and without MPFC

Figure 3.16 represents THD and FFT of voltage waveforms at the infinite bus with and without MPFC .Here Frequency (Hz) is taken on X-axis and magnitude is taken on Y-axis.

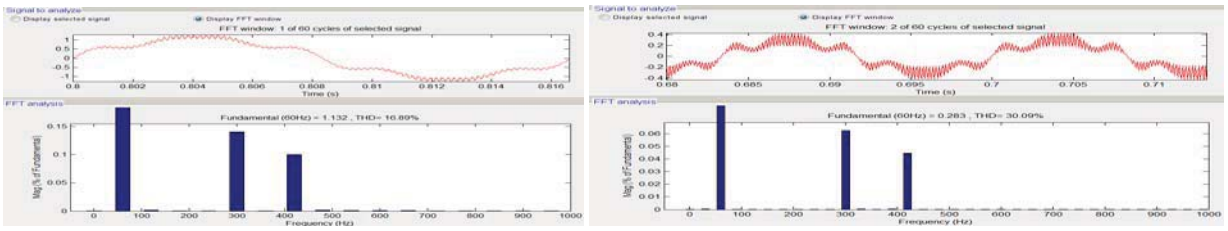

Figure 3.17: THD and FFT of current waveforms at the load bus with and without MPFC

Figure 3.17 represents THD and FFT of current waveforms at the infinite bus with and without MPFC .Here Frequency (Hz) is taken on X-axis and magnitude is taken on Y-axis.

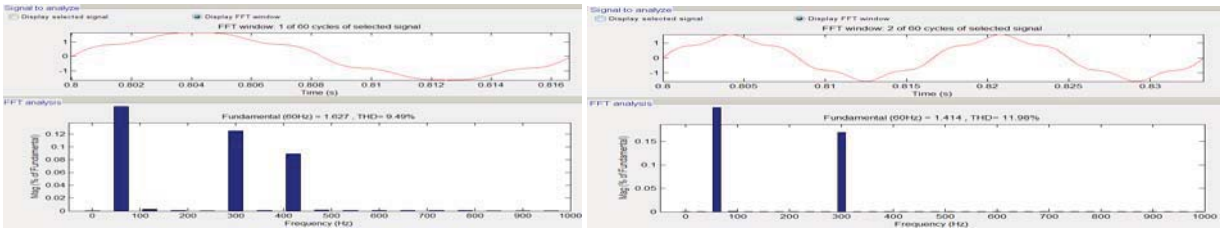

Figure 3.18: THD and FFT of voltage waveforms at the load bus with and without MPFC

Figure 3.18 represents THD and FFT of voltage waveforms at the infinite bus with and without MPFC .Here Frequency (Hz) is taken on X-axis and magnitude is taken on Y-axis.

The previous figures confirm the compensation effectiveness as well as the harmonic filtering of the proposed MPFC.

3.2 Short Circuit Fault Condition Case

A three phase short circuit (SC) fault is occurred at bus Vs, as shown in following figures, for a duration of 0.1sec, from t = 0.2 sec to t= 0.3 sec.

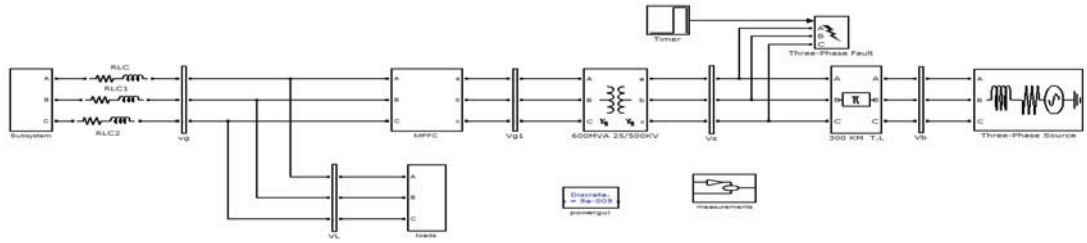

Figure 3.19: Simulation Circuit of Proposed Facts Based Dynamic Voltage Compensation Scheme with Short Circuit Fault Condition Case

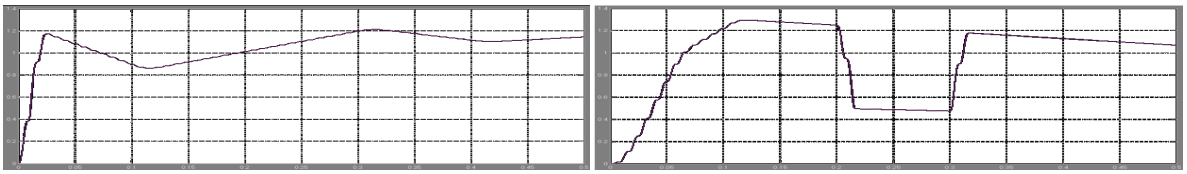

Figure 3.20: The RMS voltage at generator and load buses under short circuit (SC) fault condition at bus Vs with and without MPFC

Figure 3.202: the RMS voltage at generator and load buses under short circuit (sc) fault condition at bus Vs with and without MPFC.here time (sec) is taken on X-axis and voltage is taken on Y-axis.

In fig 3.20 (a), initially (t=0sec), there is no load so that pu Vrms increases from 0 to 1.1 pu Vrms. Linear and nonlinear load is on at 0.1sec so that pu Vrms to be approximately constant.

In fig 3.20 (b), initially (t=0sec) there is no load so that pu RMS current increases from 0 to 1.3 pu RMS current. Linear and nonlinear load is on at 0.1sec so that pu RMS current is decreased 1.3 pu to 0.6pu RMS current between 0.01 to 0.1 sec after pu RMS current to be approximately constant.

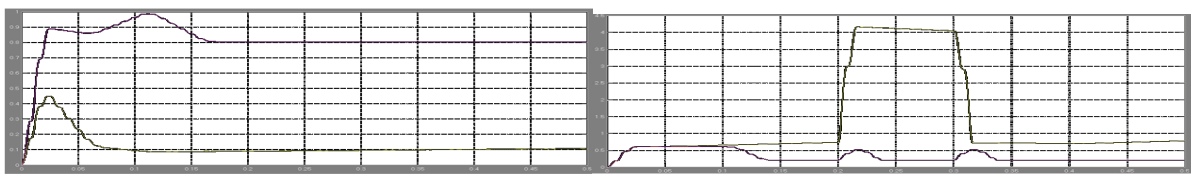

Figure 3.21: The RMS current at generator and load buses under short circuit (SC) fault condition at bus Vs with and without MPFC

Figure 3.21: the RMS current at generator and load buses under short circuit (sc) fault condition at bus Vs with and without MPFC.here time (sec) is taken on X-axis and current is taken on Y-axis.

In fig 3.21(a), initially (t=0sec) pu RMS current increases from 0 to 0.9 pu RMS current. Linear and nonlinear load is on at 0.1sec so that pu RMS current is increased 0.9 pu to 1 pu RMS current between 0.01 to 0.1 sec after pu RMS current to be approximately constant.

In fig 3.21 (b), At t=0sec, pu RMS current increases from 0 to 0.5 pu RMS current due to linear and nonlinear load pu RMS current is unbalanced between 0.01sec to 0.1sec due to MPFC pu RMS current is decreased.

3.3 Hybrid Local Load Excursions Case

The real time dynamic responses of the system for a load excursion are obtained for the following time sequences.

- At t = 0.1 sec, linear load is disconnected for a duration of 0.05 sec.

- At t = 0.2 sec, nonlinear load is disconnected for a duration of 0.05 sec.

- At t = 0.3 sec, the induction motor torque is decreased by 50% for a duration 0.05 sec.

- At t = 0.4 sec, the induction motor torque is increased by 50% for a duration 0.05 sec.

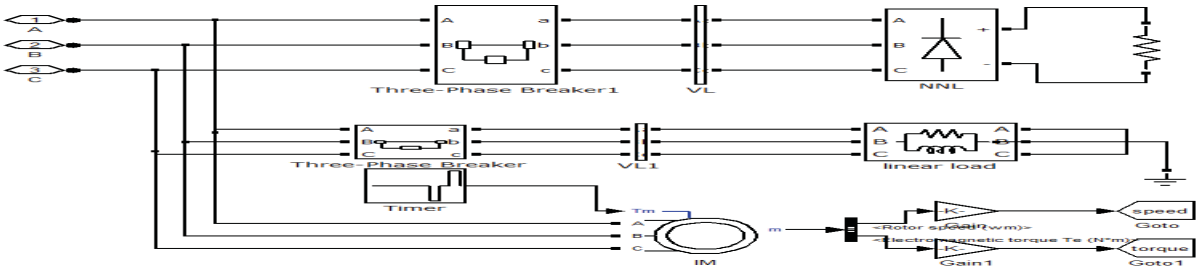

Figure 3.22: Load under Hybrid Local Load Excursions Case

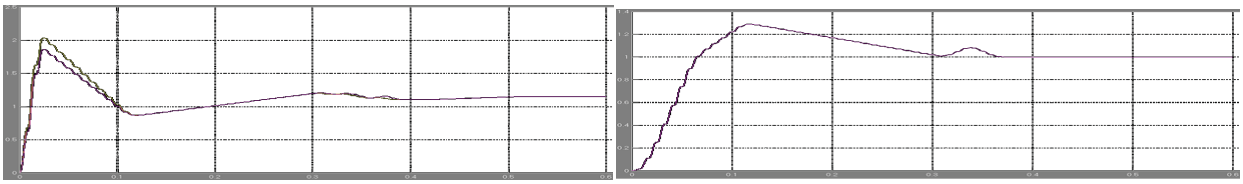

Figure 3.33: The RMS voltage waveform at the generator an d load buses under load excursions with and without MPFC

Figure 3.33: the RMS voltage at generator and load buses under load excursions at bus Vs with and without MPFC.Here Time (sec) is taken on X-axis and voltage is taken on Y-axis.

In fig 3.33 (a), initially (t=0sec) there is no load so that pu Vrms increases from 0 to 2.0 pu Vrms. Linear and nonlinear load is on at 0.1sec so that pu Vrms to be approximately constant.

In fig 3.33 (b), initially (t=0sec) there is no load so that pu RMS voltage increases from 0 to 1.3 pu RMS voltage. Linear and nonlinear load is on at 0.1sec so that pu RMS current is decreased 1.3 pu to 0.6pu RMS voltage between 0.01 to 0.1 sec after pu RMS voltage to be approximately constant.

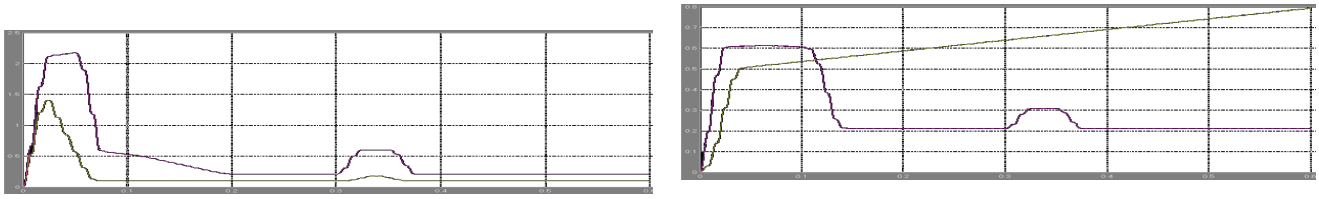

Figure 3.34: The RMS current waveform at the generator and load buses under load excursions without and with MPFC

Figure 3.34: the RMS current at generator and load buses under load excursions without and with MPFC.here time (sec) is taken on X-axis and current is taken on Y-axis.

In fig 3.34 (a), initially (t=0sec) pu RMS current increases from 0 to 2.2 pu RMS current. Linear and nonlinear load is on at 0.1sec so that pu RMS current is unbalanced after pu RMS current to be approximately constant.

In fig 3.34 (b), At t=0sec, pu RMS current increases from 0 to 0.6 pu RMS current due to linear and nonlinear load pu RMS current is unbalanced between 0.01sec to 0.1sec due to MPFC pu RMS current is approximately constant.

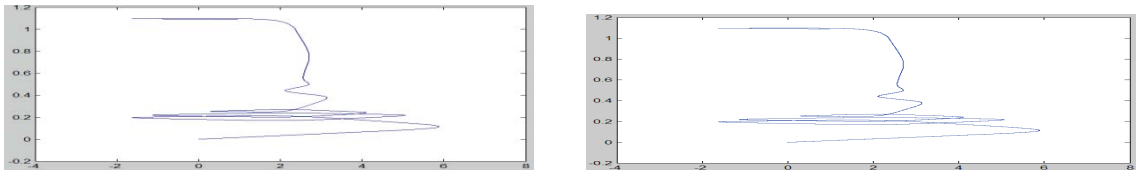

Figure 3.35: The speed-torque relationship of the induction motor without and with MPFC

Figure 3.35: The speed-torque relationship of the induction motor without and without MPFC.here torque is taken on X-axis and speed is taken on Y-axis

		P Loss	Q Loss	S Loss
Case 1 (Normal Loading Operation Case)	Without	0.0832	0.1542	0.1752
	With	0.001	0.007	0.0071
Case 2 (Short Circuit Fault Condition Case)	Without	0.1954	0.3467	0.398
	With	0.001	0.007	0.0071
Case 3 (Hybrid Local Load Excursions Case)	Without	0.1018	0.1869	0.2128
	with	0.0011	0.0065	0.0066

Table 1: The transmission line losses

Comparing the dynamic response results without and with using the proposed MPFC under three study cases; normal operation, short circuit fault conditions and hybrid load excursion, it is quite apparent that the proposed MPFC enhanced the power quality, improved power factor, compensated the reactive power, stabilized the buses voltage and reduced the transmission line losses.

IV.CONCLUSION

This paper presents a novel modulated switched power filter compensator (MPFC) scheme. The MPFC is controlled by a dynamic tri-loop dynamic error driven modified PID controller. The digital simulation model of the proposed MPFC scheme has been validated for effective power quality improvement, voltage stabilization, and power factor correction and transmission line loss reduction. The proposed FACTS based scheme can be extended to other distributed/dispersed renewable energy interface and utilization systems and can be easily modified for other specific compensation requirements, voltage stabilization and efficient utilization. Topology variations and flexible dynamic control techniques can be utilized in renewable energy smart grid interface.

In this paper, a novel FACTS based on modulated power filter compensator (MPFC), which is controlled by a novel tri-loop dynamic error driven PID controller, is simulated under different operation conditions for grid connected to wind energy conversion system. A novel tri-loop dynamic error driven PID controller developed and is used to provide voltage regulation the novel FACTS based on MPFC scheme.

The simulation results obtained from the proposed MPFC scheme has been verified for influential power factor correction, voltage regulation and energy utilization in both source bus and load bus. The proposed MPFC scheme can be quite simply used to provide voltage stabilization, requirement compensation for renewable energy sources in used distributed systems.

V.FUTURE SCOPE

In this papert, we are analyzing and reducing pu power losses and improve system stability for renewable energy source of wind power using Modulated Power Filter Compensator (MPFC).The proposed FACTS based scheme can be extended to distributed/dispersed renewable energy interface and utilization system

For future, we can also reducing the pu power losses and develop the system improvement for renewable energy sources of wind power using fuzzy logic, pspice and also neural networks.

REFERENCES

[1] A.M. Sharaf, Hassan A. Mahasneh and Yevgen Biletskiy, **"**Energy Efficient Enhancement in AC Utilization Systems" The 2007 IEEE Canadian Conference on Electrical and Computer Engineering CCECE 07, Vancouver, Canada, April 2007.
[2] A.M. Sharaf, W. Wang, and I.H. Altas, "A Novel Modulated Power Filter Compensator for Distribution Networks with Distributed Wind Energy." International Journal of Emerging Electric Power Systems. Vol. 8, Issue 3, Article 6, Aug.2007.
[3] A.M. Sharaf and Khaled Abo-Al-Ez, "A FACTS Based Dynamic Capacitor Scheme for Voltage Compensation and Power Quality Enhancement", Proceedings of the IEEEISIE 2006 Conference, Montreal, Quebec Canada, July 2006.
[4] A. Sharaf, R. Chhetri, "A novel dynamic capacitor compensator/green plug scheme for 3-phase 4-wire utilization loads", Proceeding IEEE-CCECE conference, Ottawa, Ontario, Canada 2006.
[5] A. M. Sharaf, and G. Wang, "Wind Energy System Voltage and Energy Enhancement using Low Cost Dynamic Capacitor Compensation Scheme." Proceedings of the IEEE International Conference on Electrical, Electronic and Computer Engineering. pp. 804-807, 5-7 Sept. 2004.
[6] H. Fujita and H. Akagi , "A hybrid active filter for damping of harmonic resonance in industrial power system," IEEE Trans. Power Electron., vol. 15, no. 2, pp. 215–222, Mar. 2000.
[7] J. Arrillaga, D. A. Bradley, P. S. Bodge, "Power System Harmonics", Wiley, 1985.
[8] D. Daniel Sabin and Ashok Sundaram, "Quality Enhances", IEEE Spectrum, No. 2, PP. 34-38, 1996.
[9] A. M. Sharaf, Caixia Guo and Hong Huang,"Distribution/Utilization system voltage stabilization and power quality enhancement using intelligent smart filter", UPEC'95, England, UK, 1995.
[10] M. Aredes, K. Heumann, and E. H. Watanabe, "An universal active power line conditioner," IEEE Trans. Power Delivery, vol. 13, no. 2, pp. 545–557, Apr. 1998.